IMMUNOLOGY

Tolerogenic nanoparticles induce type II collagen–specific regulatory T cells and ameliorate osteoarthritis

Hee Su Sohn[1]†, Jeong Won Choi[2]†, JooYeon Jhun[2,3], Sung Pil Kwon[1], Mungyo Jung[1], Sangmin Yong[4], Hyun Sik Na[3,5], Jin-Hong Kim[4], Mi-La Cho[2,6]*, Byung-Soo Kim[1,7,8]*

Local inflammation in the joint is considered to contribute to osteoarthritis (OA) progression. Here, we describe an immunomodulating nanoparticle for OA treatment. Intradermal injection of lipid nanoparticles (LNPs) loaded with type II collagen (Col II) and rapamycin (LNP-Col II-R) into OA mice effectively induced Col II–specific anti-inflammatory regulatory T cells, substantially increased anti-inflammatory cytokine expression, and reduced inflammatory immune cells and proinflammatory cytokine expression in the joints. Consequently, LNP-Col II-R injection inhibited chondrocyte apoptosis and cartilage matrix degradation and relieved pain, while injection of LNPs loaded with a control peptide and rapamycin did not induce these events. Adoptive transfer of $CD4^+CD25^+$ T cells isolated from LNP-Col II-R–injected mice suggested that T_{regs} induced by LNP-Col II-R injection were likely responsible for the therapeutic effects. Collectively, this study suggests nanoparticle-mediated immunomodulation in the joint as a simple and effective treatment for OA.

INTRODUCTION

Osteoarthritis (OA) is a common joint disease that involves cartilage destruction and subchondral bone sclerosis, and is accompanied by severe pain and locomotion limitations. The general treatments for OA before joint replacement include oral administration of nonsteroidal anti-inflammatory drugs (NSAIDs) and injection of hyaluronic acid within the joint (*1*). However, these treatments relieve symptoms only to a certain extent, cannot stop the progression of the disease, and often cause side effects. Autologous chondrocyte implantation can be used to regenerate cartilage in OA patients (*2*), but is costly and invasive.

OA has been traditionally considered a noninflammatory disease caused by mechanical wear of cartilage. However, recent emerging evidence has indicated that inflammation in the synovium (synovitis) also contributes to OA development (*3*, *4*). Low-grade chronic inflammation in OA is initiated by mechanical wear of cartilage and sustained via innate and adaptive immune responses (*5*). Mechanical wear of cartilage leads to the release of extracellular matrix (ECM) fragments and damage-associated molecular patterns, which induce innate immune responses such as the release of proinflammatory mediators and macrophage infiltration into OA synovium (*6*). Compared to the synovium of healthy individuals, that of OA patients contains higher numbers of inflammatory immune cells, such as M1 macrophages, type 1 helper T cells (T_H1 cells), and T_H17 cells, and lower numbers of anti-inflammatory regulatory T cells (T_{regs}) (*4*, *7*–*10*). Inflammatory immune cells propagate synovitis and further deteriorate the cartilage tissue. T cells isolated from OA patients induced autoimmune responses to autologous articular chondrocytes in vitro (*11*). Clonal expansion of antigen-specific B cells was found in patients' OA synovium (*12*). Furthermore, autoantibodies against cartilage-derived molecules, such as type II collagen (Col II), proteoglycan, and aggrecan, were found in sera and synovial fluids of OA patients (*8*, *13*, *14*). These results suggest that OA is a multiantigenic inflammatory disease and could be effectively treated by antigen-specific immunomodulation in the joint.

T_{regs} can inhibit inflammatory immune cells such as M1 macrophages and T_H1 cells through secretion of anti-inflammatory cytokines [e.g., interleukin-10 (IL-10) and transforming growth factor–β (TGF-β)] (*15*, *16*). Thus, adoptive T_{reg} transfer therapy may hold great promise for treating inflammatory diseases (*17*). For the therapy, T_{regs} specific for a desired antigen would be advantageous over polyclonal T_{regs} for the following reasons. First, adoptive transfer of polyclonal T_{regs} may cause side effects of nonspecific systemic immunosuppression through systemic secretion of anti-inflammatory cytokines (*17*, *18*). Nonspecific systemic immunosuppression may increase vulnerability to life-threatening infections and the risk of developing malignancies. T_{regs} specific for a desired antigen exert more localized and targeted immunosuppression than polyclonal T_{regs}. Second, antigen-specific T_{regs} have been proven to be functionally superior to polyclonal T_{regs} in animal models (*19*, *20*). This would be ascribed to localization and activation of antigen-specific T_{regs} at the target site through interactions with antigen presented by antigen-presenting cells (APCs) at the inflammation site. However, broad clinical applications of adoptive transfer of autologous T_{regs} would be limited by the costly and complicated procedures of ex vivo T_{reg} manufacturing (*17*). In this context, in vivo induction of OA antigen-specific T_{regs} may show potential for OA treatment and may be

[1]School of Chemical and Biological Engineering, Seoul National University, Seoul 08826, Republic of Korea. [2]The Rheumatism Research Center, Catholic Research Institute of Medical Science, The Catholic University of Korea, Seoul 06591, Republic of Korea. [3]Department of Biomedicine and Health Sciences, College of Medicine, The Catholic University of Korea, 222, Banpo-daero, Seocho-gu, Seoul 06591, Republic of Korea. [4]Department of Biological Sciences, College of Natural Sciences, Seoul National University, Seoul 08826, Republic of Korea. [5]Lab of Translational ImmunoMedicine, Catholic Research Institute of Medical Science, College of Medicine, The Catholic University of Korea, Seoul 06591, Republic of Korea. [6]Department of Medical Life-science, College of Medicine, The Catholic University of Korea, 222, Banpo-daero, Seocho-gu, Seoul 06591, Republic of Korea. [7]Institute of Chemical Processes, Institute of Engineering Research, BioMAX, Seoul National University, Seoul 08826, Republic of Korea. [8]Interdisciplinary Program for Bioengineering, Seoul National University, Seoul 08826, Republic of Korea.
*Corresponding author. Email: iammila@catholic.ac.kr (M.-L.C.), byungskim@snu.ac.kr (B.-S.K.)
†These authors contributed equally to this work.

advantageous over adoptive transfer of OA antigen-specific T_{regs} or polyclonal T_{regs}.

Here, we present an off-the-shelf approach for OA treatment, which involves nanoparticle-mediated in vivo induction of Col II–specific T_{regs} (Fig. 1A). In vivo induced Col II–specific T_{regs} may ameliorate inflammation at the OA joint and inhibit OA progression. Col II was selected as the antigen for induction of antigen-specific T_{regs}. Col II is a major component of cartilage ECM and a potential autoantigen because autoantibodies against Col II are found in the synovial fluid and serum in OA patients (*21*). Col II present in the OA joint is susceptible to modification by inflammatory molecules, such as proteolytic enzymes and reactive oxygen species (*22*), and the modification potentially increases its antigenicity (*8*, *11*, *12*, *23*–*25*). Thus, we used Col II that was degraded by a proteolytic enzyme as the antigen to induce Col II–specific T_{regs}. The hypothesis of our approach (Fig. 1A) is as follows. Intradermally injected lipid nanoparticles (LNPs) loaded with Col II and rapamycin (LNP-Col II-R) are taken up by dendritic cells (DCs). DCs subsequently differentiate into tolerogenic DCs (tDCs) due to rapamycin, present Col II on major histocompatibility complex class II (MHC II), migrate to adjacent lymph nodes, and induce Col II–specific T_{regs}. Col II–specific T_{regs} migrate to the site of inflammation (i.e., OA joint) and are activated

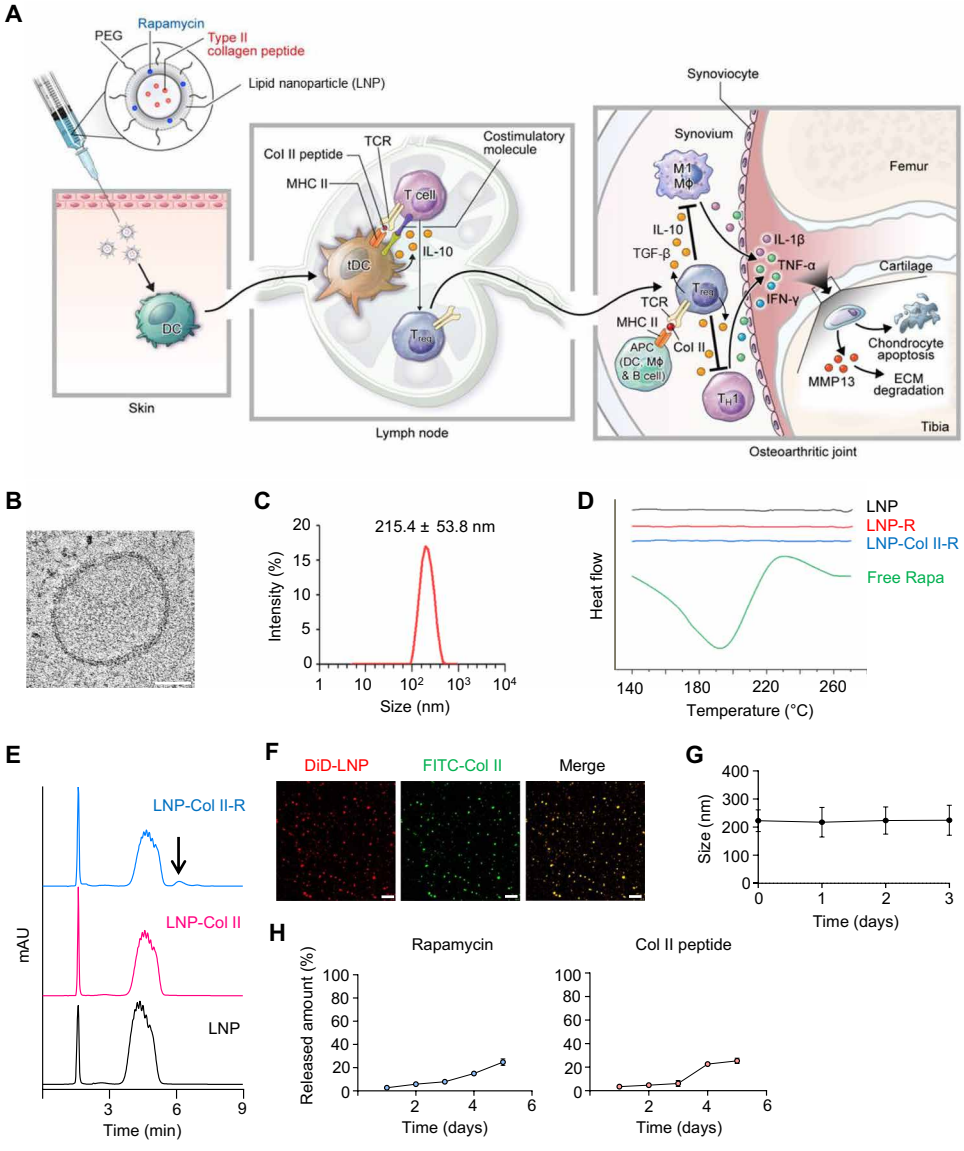

Fig. 1. The hypothesis of this study and characterization of LNPs loaded with type II collagen peptide (Col II) and rapamycin (LNP-Col II-R). (**A**) Hypothesis of this study. Intradermal injection of LNP-Col II-R to OA mice would induce Col II–specific T_{regs}. The T_{regs} in the synovium would inhibit M1 macrophages and T_H1 cells, both of which express inflammatory cytokines (e.g., TNF-α, IFN-γ, and IL-1β) and inhibit chondrocyte apoptosis and matrix destruction in the OA articular cartilage. (**B**) TEM image and (**C**) size distribution of LNP-Col II-R. Scale bars, 50 nm. Confirmation of rapamycin loaded in LNP, as evaluated by (**D**) DSC and (**E**) HPLC. The arrow indicates rapamycin peak. (**F**) Confirmation of Col II loaded in LNP by confocal microscopic photographs of LNP-Col II-R. Scale bars, 1 μm. (**G**) Colloidal stability of LNP-Col II-R in 50% (v/v) serum, as evaluated by DLS ($n = 3$). (**H**) Confirmation of released amount of Col II peptide and rapamycin from LNP-Col II-R by BCA protein assay and HPLC, respectively ($n = 3$).

upon interaction with Col II presented on MHC II of APCs (e.g., activated B cells, DCs, and macrophages) at the OA synovium. The activated T_{regs} ameliorate joint inflammation. We tested this hypothesis in a murine OA model.

RESULTS

Characterization of LNP-Col II-R

Col II for LNP-Col II-R was prepared through collagenase treatment of undenatured Col II proteins. The molecular weights of undenatured Col II proteins ranged from 13 to 100 kDa, while those of Col II after collagenase treatment ranged from 6 to 16 kDa (fig. S1). LNP-Col II-R exhibited a round morphology (Fig. 1B) and an average size of 215.4 ± 53.8 nm (Fig. 1C). LNP-Col II-R showed a positive surface charge of 6.2 ± 3.6 mV due to the cationic lipid 1,2-dioleoyl-3-trimethylammonium-propane (chloride salt) (DOTAP) of LNP. Differential scanning calorimetry (DSC) analysis revealed incorporation of rapamycin in LNP-Col II-R (Fig. 1D). The thermogram of free rapamycin crystals showed an endothermic peak at ~190°C (*26*). The peak was not observed in rapamycin-loaded LNPs (LNP-R and LNP-Col II-R) or in blank LNPs, indicating that rapamycin was incorporated into LNPs and existed in an amorphous state in the lipid bilayer of the LNPs. High-performance liquid chromatography (HPLC) analysis confirmed that rapamycin was loaded in LNP-Col II-R (Fig. 1E). The rapamycin loading efficiency was 65.9%. Confocal microscopic analysis revealed that Col II was incorporated in LNPs (Fig. 1F). LNP-Col II-R showed colloidal stability in 50% (v/v) serum for at least 3 days (Fig. 1G). Considering that DCs engulf nanoparticles within 24 hours after intradermal injection (*27*, *28*), LNP-Col II-R that is stable for 3 days would be appropriate for DC uptake after intradermal injection. Less than only 10% of rapamycin and Col II peptides were released from LNP-Col II-R within 72 hours (Fig. 1H). The slow release profiles ensure that the payloads (rapamycin and Col II) are released intracellularly. LNP-Col II-R can be internalized into endosomes of DCs by endocytosis. Subsequently, the payloads are released to the cytosol via LNP fusion with endosomal membranes (*29*, *30*). The fusion is mediated by the interactions between cationic lipids of LNPs and anionic endosomal membranes. The intracellular release leads to induction of Col II–presenting tDCs (*31*). In this context, the design of nanoparticles would be appropriate for induction of tDCs.

LNP-Col II-R–mediated antigen presentation on DCs

To determine whether LNPs enhance Col II (antigen) delivery to DCs and subsequent antigen presentation on DCs, free Col II or LNP-Col II-R was added to DC cultures. After 24 hours, 91.8% of the DCs engulfed the LNPs (Fig. 2A). In addition, LNP-Col II-R enhanced Col II delivery to DCs compared with free Col II (Col II–bearing DCs: 93.3% versus 2.2%) (Fig. 2B). Most of the Col II was presented on the DC surface in the LNP-Col II-R injection group. To determine whether antigen delivery with LNPs leads to antigen presentation on MHC II of DCs, LNPs were loaded with Eα peptides and rapamycin, and then added to DC cultures. Technically, the presentation of Col II on MHC II of DCs is difficult to prove directly. Thus, we exploited the Yae antibodies that bind to both the Eα peptide and MHC II simultaneously, and indirectly demonstrated Eα peptide (antigen) presentation on MHC II following the addition of LNP-Eα-R to DC cultures (Fig. 2C). The addition of LNP-Eα-R led to 82.0% of the DCs presenting Eα peptide on MHC II. In contrast, the addition of free Eα peptides to DC cultures resulted in only 17.1% of the DCs presenting Eα peptide on MHC II.

LNP-Col II-R–mediated induction of tDCs

tDC can induce naïve T cells to differentiate into T_{regs}. To determine whether LNP-Col II-R can induce tDCs, DCs were cultured in the presence of different types of LNPs for 48 hours and subsequently activated by lipopolysaccharide (LPS) for 24 hours. Rapamycin, an immunosuppressive agent, is known to endow DCs with tolerogenic properties (*31*). Flow cytometry analysis indicated that mature DCs (mDCs) expressed costimulatory surface molecules (CD40, CD80, and CD86) and MHC II at higher levels than immature DCs (iDCs) (Fig. 2D). The costimulatory molecule levels of LNP-Col II-R– and LNP-R–treated DCs were significantly higher than those of iDCs and lower than those of LNP-Col II–treated DCs and mDCs. Quantitative reverse transcription polymerase chain reaction (qRT-PCR) analysis showed that mDCs expressed the highest mRNA levels of inflammatory cytokine, tumor necrosis factor–α (TNF-α), and the lowest mRNA level of anti-inflammatory cytokine, TGF-β, compared with the other groups (Fig. 2E). The mRNA level of TNF-α in LNP-Col II-R–treated DCs was higher than that of iDCs and lower than those of LNP-Col II–treated DCs and mDCs. The TGF-β mRNA level of LNP-Col II-R–treated DCs was significantly higher than those of iDCs, LNP-Col II–treated DCs, and mDCs. Together, these data indicate that LNP-Col II-R treatment to DCs can induce tDCs. The enzyme-linked immunosorbent assay (ELISA) data showed that LNP-Col II-R–treated DCs secreted more anti-inflammatory cytokine (TGF-β) than iDCs and mDCs, and less inflammatory cytokine (TNF-α) than mDCs (Fig. 2F).

Biodistribution of nanoparticles after intradermal injection

To examine the biodistribution of LNP-Col II-R after intradermal injection, LNPs were labeled with 1,1′-dioctadecyl-3,3,3′,3′-tetramethylindotricarbocyanine iodide (DiR), a lipophilic dye, and then intradermally injected near the right inguinal lymph node (iLN) of mice. In vivo imaging at 6, 24, and 48 hours after injection revealed that the nanoparticles existed near the injection site for at least 48 hours (Fig. 3A). DCs are known to engulf foreign particles within 24 hours (*27*, *28*). At 24 hours, the DiR-labeled nanoparticles were observed only in the right iLNs and not in the major organs (Fig. 3B). The in vivo biodistribution study of free rapamycin could not be conducted because it is difficult to label rapamycin with fluorescent dye. Instead, we conducted a biodistribution study using a fluorescent molecule, DiR, which has a similar hydrophobic property to that of rapamycin. Free DiR molecules dispersed in vivo after intradermal injection near the right iLN, and fluorescence was not detected near the injection site 2 hours after injection and in the major organs and the right iLN 24 hours after injection (fig. S2, A and B). These results suggest that intradermal injection of free rapamycin might not be suitable for local delivery to lymph node. Immunostaining of the right iLNs retrieved at 24 hours revealed that DCs ($CD11c^+$ cells) contained LNPs (Fig. 3C) and interacted with $CD3^+$ T cells in paracortex of the lymph node (Fig. 3, C and D).

LNP-antigen-R–mediated induction of antigen-specific T_{regs}

Given that LNP-R can induce tDCs (Fig. 2, D and E), we next investigated whether LNP-antigen-R can induce antigen-specific T_{regs} both in vivo and in vitro. Considering that $CD4^+$ T cells of OT-II transgenic mice are highly responsive to chicken ovalbumin 323 to

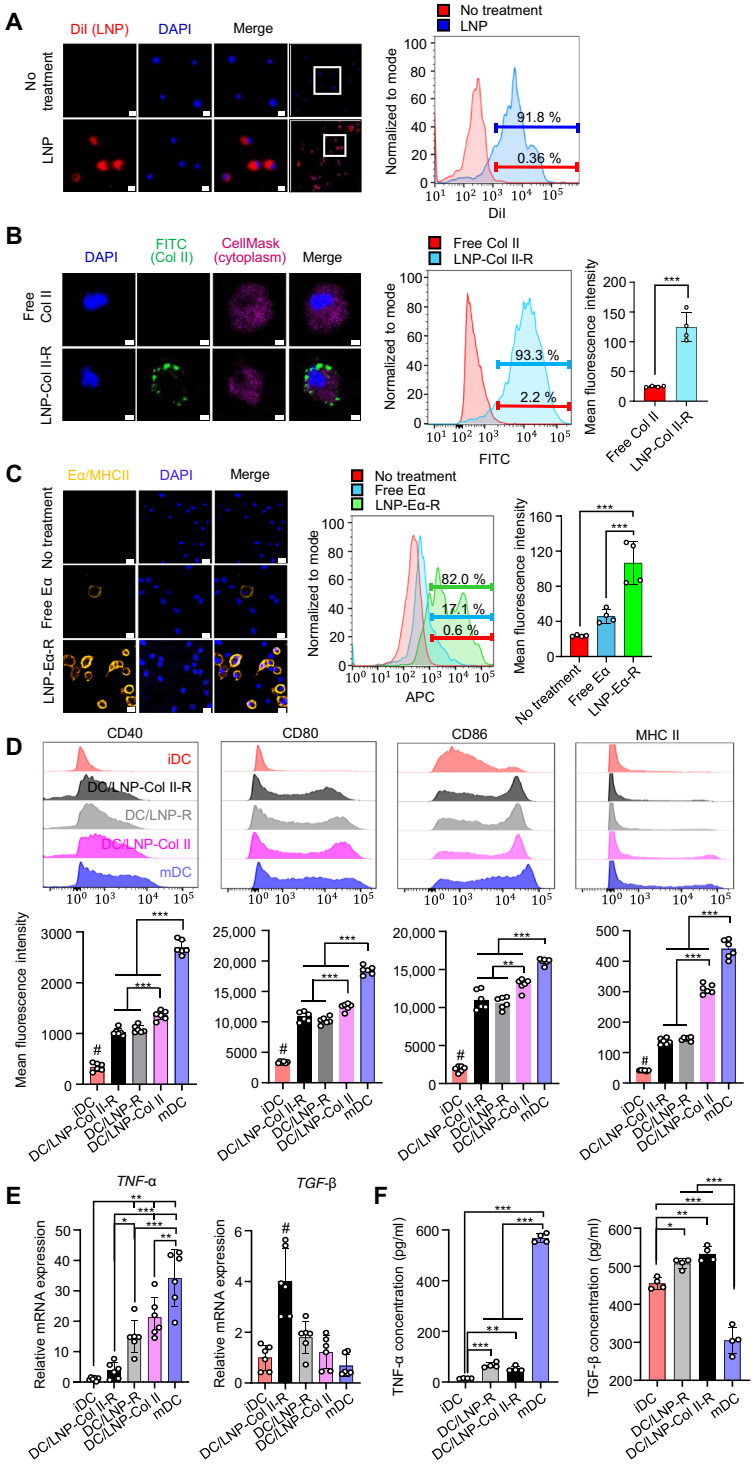

Fig. 2. LNP-Col II-R–mediated antigen presentation on DCs and subsequent induction of tDCs in vitro. (**A**) Effective uptake of LNPs by DCs in vitro. Scale bars, 50 μm. (**B**) LNP-Col II-R–mediated, effective presentation of antigen (Col II) on DCs in vitro. Scale bars, 10 μm ($n = 4$). (**C**) LNP-mediated, effective presentation of antigen (Eα peptide) on MHC class II of DC surface in vitro. Scale bars, 50 μm ($n = 4$). LNP-Col II-R–mediated, effective induction of tDCs in vitro, as evaluated by DC surface protein analyses with (**D**) flow cytometry ($n = 6$), (**E**) cytokine mRNA analysis with qRT-PCR ($n = 6$), and (**F**) ELISA ($n = 4$). (B) ***$P < 0.001$. Two-tailed t test. (C to E) $^{\#}P < 0.001$ versus any group, *$P < 0.05$, **$P < 0.01$, and ***$P < 0.001$. One-way ANOVA (multiple comparison) with Tukey's post hoc test.

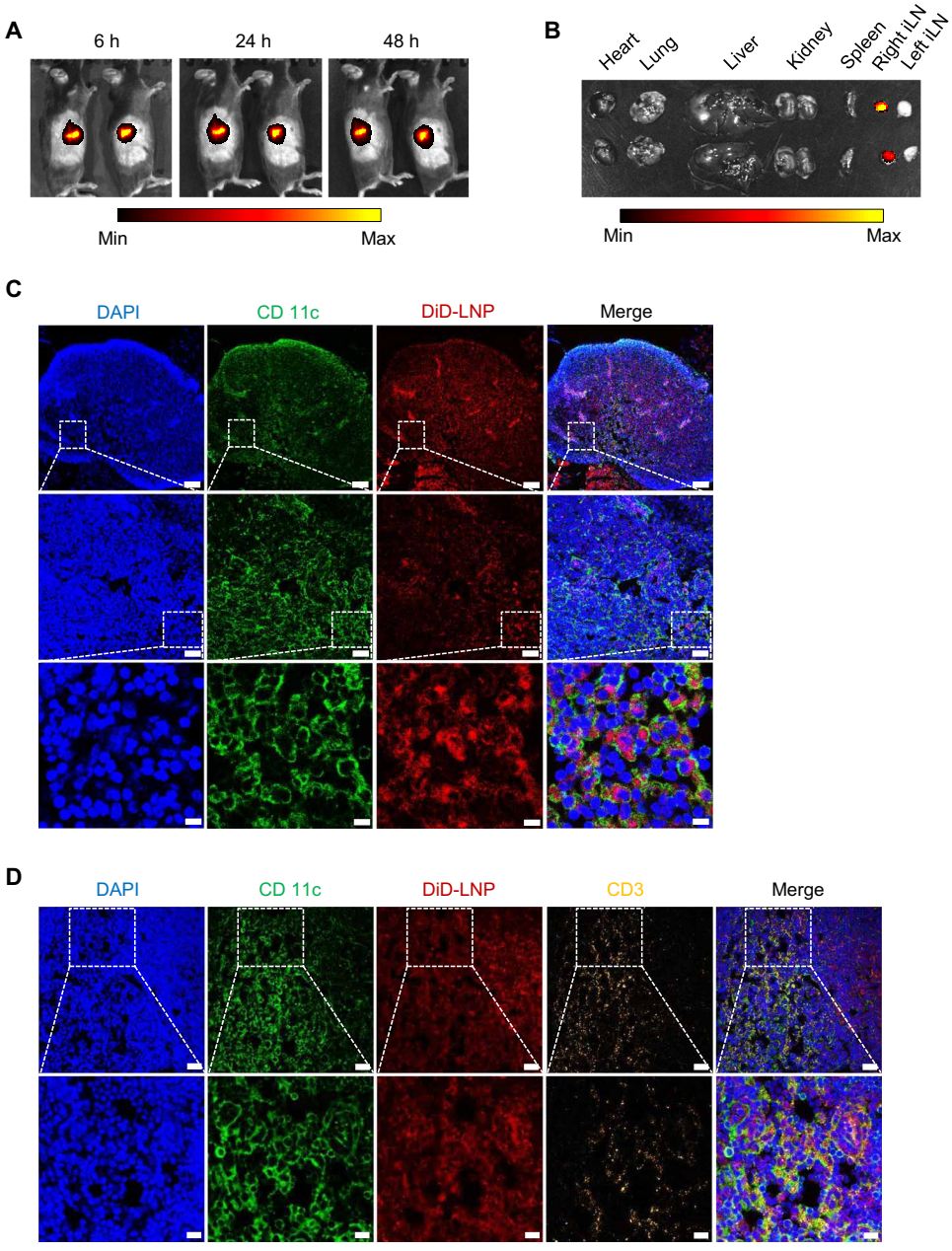

Fig. 3. Biodistribution of LNP-Col II-R after intradermal injection. (**A**) Fluorescence intensity of DiR-labeled LNP-Col II-R at 6, 24, and 48 hours after intradermal injection near the right iLN of mice. (**B**) Fluorescence intensity of major organs and iLN 24 hours after intradermal injection near the right iLN. (**C**) Immunostaining of DCs in the right iLN with anti-CD11c antibodies 24 hours after intradermal injection of DiD-labeled LNP-Col II-R, indicating colocalization of LNP-Col II-R and DCs in the right iLN. The photographs of the lowest row are a higher magnification of the rectangular areas (paracortex) of those in the top rows. Scale bars, 100 μm (top row), 50 μm (middle row), and 5 μm (bottom row). (**D**) Immunostaining of DCs and T cells in the right iLN with anti-CD11c and anti-CD3 antibodies 24 hours after intradermal injection of DiD-labeled LNP-Col II-R, indicating colocalization of LNP-Col II-R, DCs, and T cells in the right iLN. The photographs of the bottom row are a higher magnification of the rectangular areas of those in the top row. Scale bars, 50 μm (top row) and 10 μm (bottom row).

339 peptides (OVA), LNPs loaded with different types of molecules were injected intradermally into OT-II mice to assess the ability of LNPs loaded with OVA to induce OVA-specific T_{regs} in vivo (Fig. 4A). LNP-OVA-R injection resulted in a significantly higher proportion of OVA-specific T_{regs} in the iLNs than the other types of nanoparticles including LNP-R, LNP-Col II-R, and LNP-OVA. Next, we evaluated the ability of DCs harboring LNP-antigen-R nanoparticles to activate and expand antigen-specific T_{regs} in vitro (Fig. 4B). DCs were treated with different types of LNPs in vitro and subsequently cocultured with $CD4^+$ T cells isolated from OT-II transgenic mice. The LNP-OVA-R group showed significantly higher activation of T_{regs} than the other groups. Next, we investigated whether intradermal injection of LNP-Col II-R generates Col II–specific T_{regs} in OA wild-type mice. LNPs loaded with different types of molecules were injected

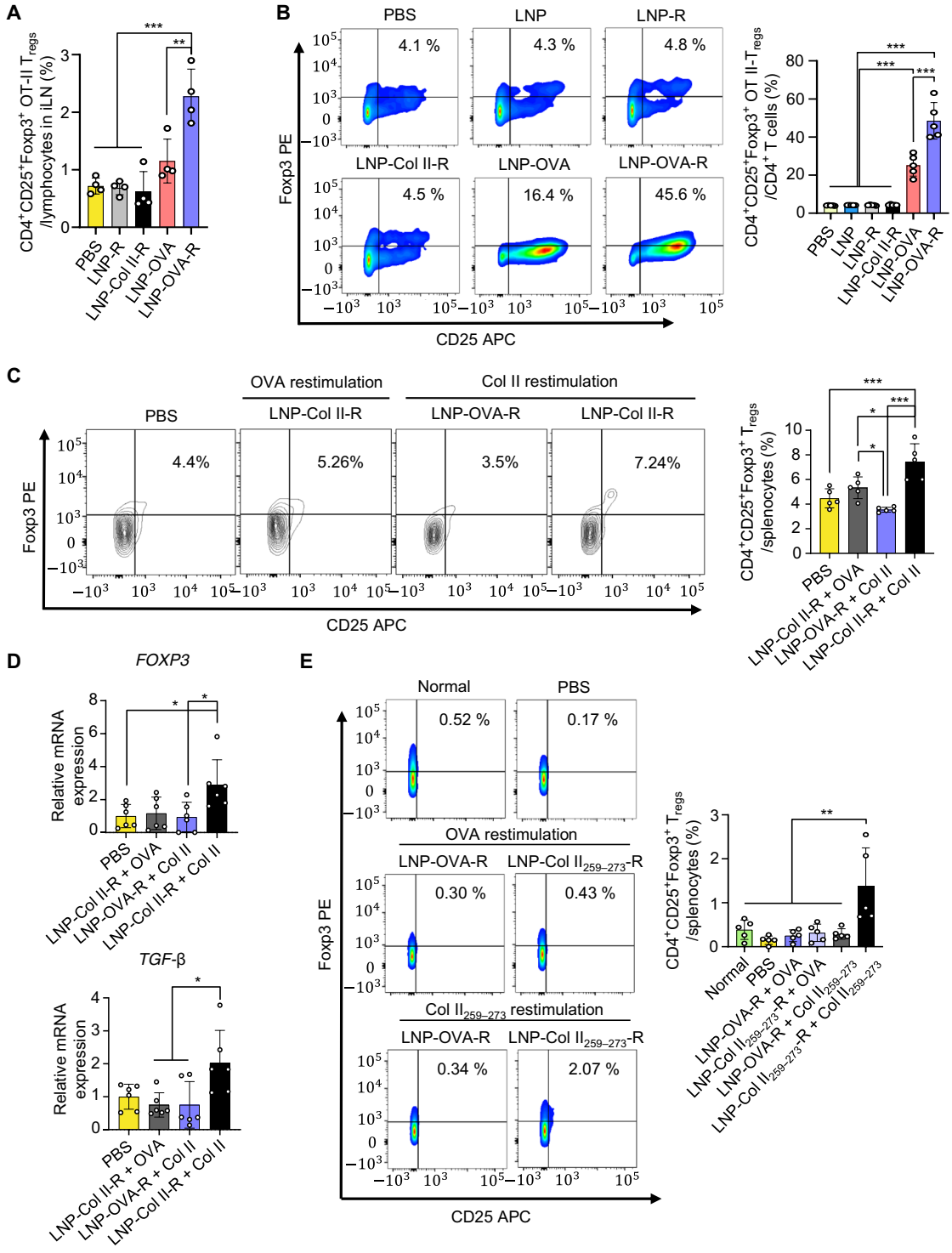

Fig. 4. In vitro and in vivo generation of antigen-specific T_{regs} by nanoparticles. (**A**) Proportion of OVA-specific T_{regs} in iLN following intradermal injection of different types of nanoparticles to OT-II transgenic mice that have T cells specific for OVA only, as evaluated by flow cytometry ($n = 4$). (**B**) Proportion of T_{regs} generated in vitro from OT-II $CD4^+$ T cells following coculture of the $CD4^+$ T cells with DCs that had been treated with various types of nanoparticles in vitro ($n = 5$). (**C**) Proportion of T_{regs} in splenocytes. The splenocytes were isolated from wild-type OA mice that had been treated with intradermal injection of different types of nanoparticles and subsequently restimulated in vitro with Col II or OVA ($n = 5$). (**D**) Relative mRNA expression of FOXP3 and TGF-β in the splenocytes restimulated in vitro with Col II or OVA ($n = 6$). (**E**) Proportion of T_{regs} in splenocytes analyzed by flow cytometry. The splenocytes were isolated from wild-type OA mice that had been treated with intradermal injection of different types of nanoparticles and subsequently restimulated in vitro with Col $II_{259–273}$ (epitope) or OVA ($n = 5$). (A to E) $^*P < 0.05$, $^{**}P < 0.01$, and $^{***}P < 0.001$. One-way ANOVA (multiple comparison) with Tukey's post hoc test.

into the mice. Then, splenocytes were harvested and treated with Col II or OVA for antigen-specific restimulation. The LNP-Col II-R group restimulated with Col II showed the highest proportion of T_{regs} (Fig. 4C) and the highest mRNA expressions of T_{reg}-specific genes, forkhead box p3 (Foxp3) and TGF-β (Fig. 4D). The well-known epitope for Col II is Col $II_{259–273}$. Col $II_{259–273}$ is known to be loaded on MHC II and aggravate rheumatoid arthritis by activating Col $II_{259–273}$-specific $CD4^+$ T cells (*32*). We examined the feasibility of Col $II_{259–273}$ epitope for in vivo generation of Col $II_{259–273}$-specific T_{regs}. After intradermal injection of LNP-Col $II_{259–273}$-R or LNP-OVA-R to mice, splenocytes were harvested and treated with Col $II_{259–273}$ or OVA in vitro for T_{reg} restimulation. The LNP-Col $II_{259–273}$-R group showed the highest proportion of T_{regs} (Fig. 4E). Collectively, these data indicate that LNP-Col II-R can generate Col II–specific T_{regs}.

Therapeutic effects of LNP-Col II-R in OA mice

To evaluate the therapeutic effects of LNP-Col II-R, C57BL/6 mice underwent destabilization of medial meniscus (DMM) surgery on the right side of the knee for OA induction, and the left knee remained as a control (*33*). The level of autoantibodies against Col II in murine DMM-induced OA model was determined with ELISA after 8 weeks of DMM surgery (Fig. 5A). The level of Col II immunoglobulin G (IgG) increased in the DMM-induced mouse model as compared to the normal healthy group. For the treatment, the nanoparticles were injected intradermally on the right side of the dorsal flank near the iLN. At week 8, Safranin O–Fast Green staining of the joints qualitatively showed that DMM surgery induced cartilage destruction and that LNP-Col II-R injection inhibited cartilage destruction more effectively than the other groups (Fig. 5B). The Osteoarthritis Research Society International (OARSI) score of the LNP-Col II-R group was significantly lower than those of the other groups (Fig. 5C and fig. S4). The size and maturity of osteophytes in the Safranin O–Fast Green staining images (Fig. 5D) were quantified according to the scoring system (Fig. 5E) (*34*, *35*). The LNP-R or LNP-Col II-R injection groups showed smaller size and lower maturity of osteophytes compared with other groups. The synovitis was analyzed by hematoxylin and eosin (H&E) staining of the joint synovium (Fig. 5F). The synovial lining of the joints showed a higher extent of immune cell infiltration after DMM surgery, in agreement with a previous study (*36*). The LNP-Col II-R injection group showed a lower degree of immune cell infiltration than the other groups. Terminal deoxynucleotidyl transferase–mediated deoxyuridine triphosphate nick end labeling (TUNEL) staining data at 8 weeks indicated that chondrocyte apoptosis was highly increased in all groups except for the LNP-Col II-R group as compared to the normal healthy group (Fig. 5G). Col II in the cartilage was maintained at a higher level in the LNP-Col II-R–injected mice (Fig. 5, H and I). This is likely due to the decreased expression of matrix metalloproteinase 13 (MMP13) (Fig. 5, H and I), which degrades Col II, and the higher expression of Col II in the LNP-Col II-R–injected mice (Fig. 5J). The lower level of Col II in the cartilage of the LNP group is likely due to the increased MMP13 expression and decreased Col II expression. The normal group was used as the control in this study instead of the sham surgical group. Because the OARSI scores of the normal and sham surgical control groups were not different from each other (fig. S3), the lack of the sham surgical control would not affect the evaluation of the therapeutic efficacy. At week 8, the animals' pain was evaluated by the mechanical allodynia test (von Frey test) and static weight-bearing test. The von Frey test measures the withdrawal force at which stimulation to the hind paw causes pain such that the animals withdraw their hind paw from the plate. The withdrawal force threshold of the LNP-Col II-R group was significantly higher than those of the other groups and similar to that of the normal healthy group (Fig. 5K). The weight-bearing test showed that LNP-Col II-R injection more effectively relieved pain than injection of phosphate-buffered saline (PBS), LNP, or LNP-OVA-R (Fig. 5L). Pain relief by LNP-Col II-R injection is likely due to mitigated inflammation in the joint (*37*).

LNP-Col II-R–mediated immunomodulation in the synovium of OA mice

Inflammatory immune cells infiltrate the synovium of OA joint and are intimately involved in the progression of OA (*5*, *7*, *10*, *13*, *24*, *37–40*). We investigated whether LNP-Col II-R injection could mitigate inflammation at the OA joint by modulating inflammatory immune cells in the synovium. Immunostaining analyses indicated that LNP-Col II-R injection significantly increased T_{regs} in the synovium at 8 weeks compared with the other treatments (Fig. 6A). Meanwhile, immunostaining for a macrophage marker (F4/80) and an M1 macrophage marker [inducible nitric oxide synthase (iNOS)] indicated that LNP-Col II-R injection significantly reduced the number of inflammatory M1 macrophages in the synovium compared to the other treatments (Fig. 6B). The number of anti-inflammatory M2 macrophages in the synovium was not significantly different among the LNP-Col II, LNP-R, and LNP-Col II-R groups (fig. S5). Moreover, LNP-Col II-R injection reduced the densities of interferon-γ (IFN-γ)–secreting $CD4^+$ T cells, IL-17–secreting $CD4^+$ T cells, and IL-1β–secreting M1 macrophages in the synovium (Fig. 6, C and D, and fig. S6). These results may be ascribed to the LNP-Col II-R injection–mediated increase in the number of anti-inflammatory IL-10–secreting T_{regs} in the synovium (Fig. 6E) that inhibit inflammatory $CD4^+$ T cells and M1 macrophages. PCR analyses showed tendencies for the expression of IFN-γ, IL-1β, TNF-α, and TGF-β in the joints (Fig. 6F), which were similar to the immunostaining results. LNP-Col II-R injection significantly decreased the mRNA expression of inflammatory cytokines (IFN-γ, IL-1β, and TNF-α) and increased that of the anti-inflammatory cytokine TGF-β in the OA joints.

Therapeutic effects of adoptive cell transfer to OA mice

To investigate whether T_{regs} induced by LNP-Col II-R injection are responsible for the therapeutic effects, we performed adoptive T cell transfer to OA mice. $CD4^+CD25^+$ T cells that included T_{regs} were isolated from the spleens of mice that had been treated with intradermal injection of PBS, LNP-R, or LNP-Col II-R. The reason for sorting cells with only CD4 and CD25 without Foxp3 is to retain the cells' therapeutic effect. To isolate $Foxp3^+$ T_{regs}, a cell permeabilizing step is necessary, which would kill the cells and make the cells unsuitable for the adoptive transfer (*41*). In adoptive T_{reg} transfer in clinical trials, therefore, $CD4^+CD25^+CD127^-$ or $CD4^+CD25^+CD127^-CD45RA^+$ T cells are sorted and transferred (*18*), while $CD4^+CD25^+$ T cells are sorted in murine model for adoptive T_{reg} transfer (*42*). The isolated $CD4^+CD25^+$ T cells were transferred to OA mice by intravenous injection (Fig. 7A). Safranin O–Fast Green staining of the joints at 8 weeks indicated that the LNP-Col II-R group showed less destruction in the cartilage and scored significantly lower OARSI grades than the other groups (Fig. 7B). Immunostaining analysis indicated that the number of $CD4^+CD25^+Foxp3^+$ T_{regs} in the synovium was significantly higher in the LNP-Col II-R group than in

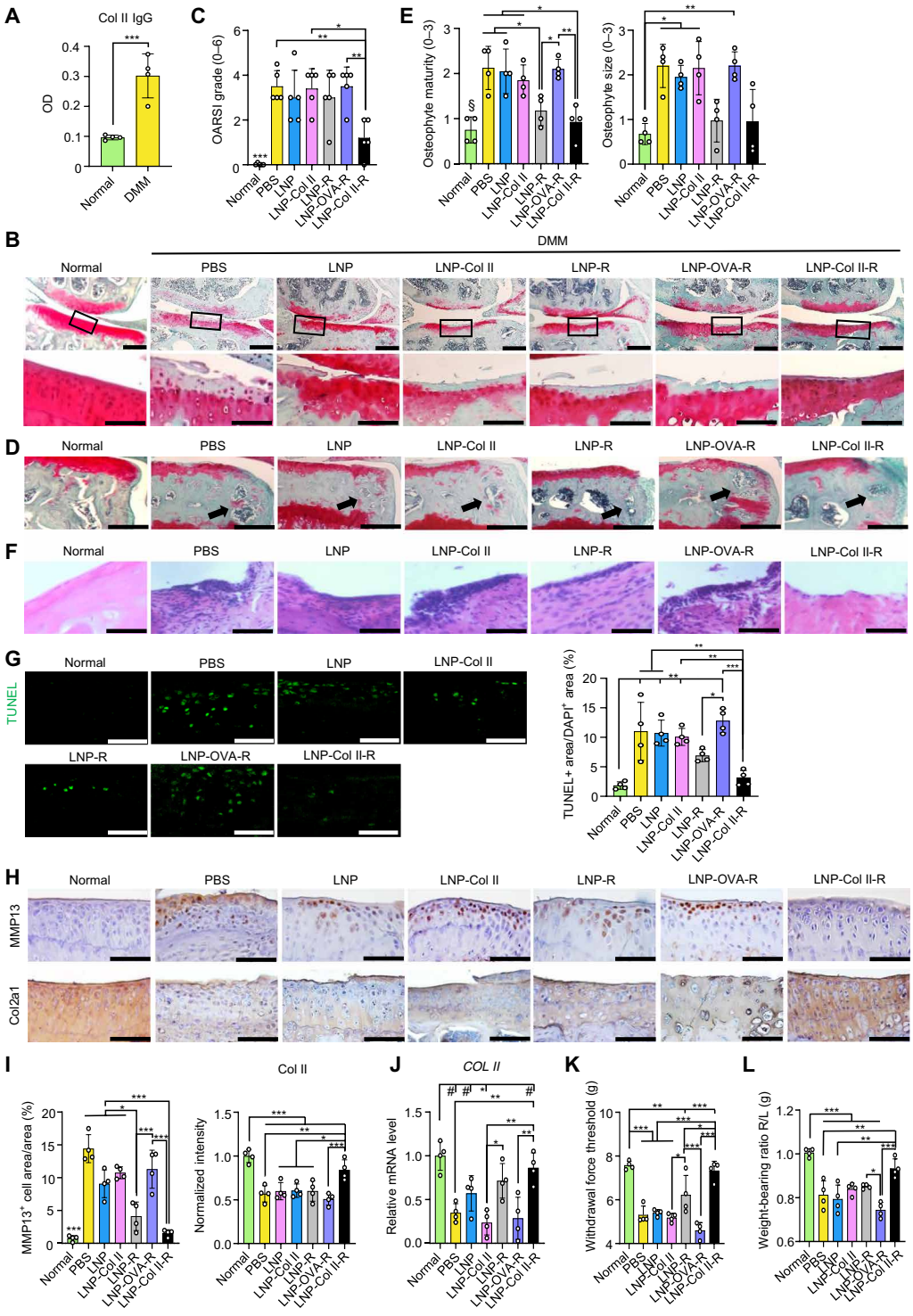

Fig. 5. Therapeutic effects of LNP-Col II-R in OA mice at 8 weeks. (**A**) Level of autoantibodies against Col II in serum of DMM-induced mice ($n = 4$). (**B**) Representative Safranin O–Fast Green–stained sections of the joints. Photographs of the bottom row are higher magnification of the rectangular areas of those in the top row. Scale bars, 100 μm. (**C**) OARSI scores. *$P < 0.05$, **$P < 0.01$, and ***$P < 0.001$ versus any group except LNP-Col II-R. One-way ANOVA with Tukey's post hoc test ($n = 5$). (**D**) Representative Safranin O–Fast Green–stained sections of the joints. The osteophytes are indicated with black arrows. Scale bars, 100 μm. (**E**) Osteophyte size and maturity analysis. *$P < 0.05$, **$P < 0.01$, and $^{§}P < 0.001$ versus any group except LNP-R and LNP-Col II-R. One-way ANOVA with Tukey's post hoc test ($n = 4$). (**F**) H&E staining of the synovium. Scale bars, 100 μm. (**G**) TUNEL staining of the cartilage. Scale bars, 100 μm. (**H**) Immunostaining for MMP13 and Col2a1 in the cartilage (scale bars, 100 μm) and (**I**) quantification. (**J**) Relative mRNA expressions of Col II in the joints ($n = 4$). Pain evaluated by (**K**) mechanical allodynia (von Frey) test and (**L**) static weight-bearing test. (A, G, and I to L) *$P < 0.05$, **$P < 0.01$, and ***$P < 0.001$. One-way ANOVA (multiple comparison) with Tukey's post hoc test ($n = 4$).

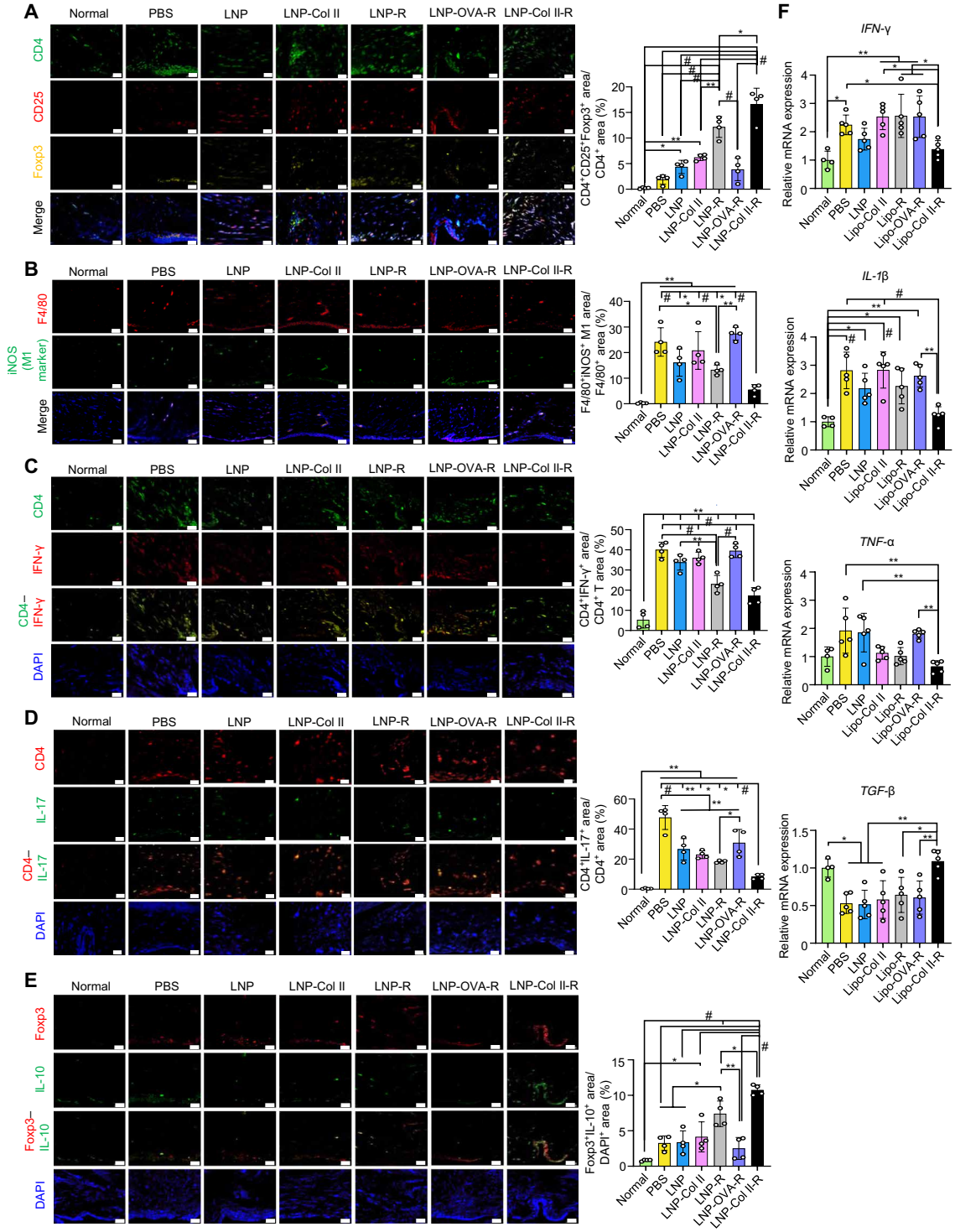

Fig. 6. Immunomodulation in the synovium of OA mice at 8 weeks. Immunostaining for (**A**) $CD4^+CD25^+Foxp3^+$ T_{regs}, (**B**) $F4/80^+iNOS^+$ M1 macrophages, (**C**) $CD4^+IFN\text{-}\gamma^+$ T cells, (**D**) $CD4^+IL\text{-}17^+$ T cells, and (**E**) $Foxp3^+IL\text{-}10^+$ T_{regs} in the synovium. (**F**) Relative mRNA expressions of IFN-γ, IL-1β, TNF-α, and TGF-β in the joints. $n = 5$ except for the normal group ($n = 4$). (A to E) Scale bars, 20 μm ($n = 4$). (A to F) $^*P < 0.05$, $^{**}P < 0.01$, and $^{\#}P < 0.001$. One-way ANOVA (multiple comparison) with Tukey's post hoc test.

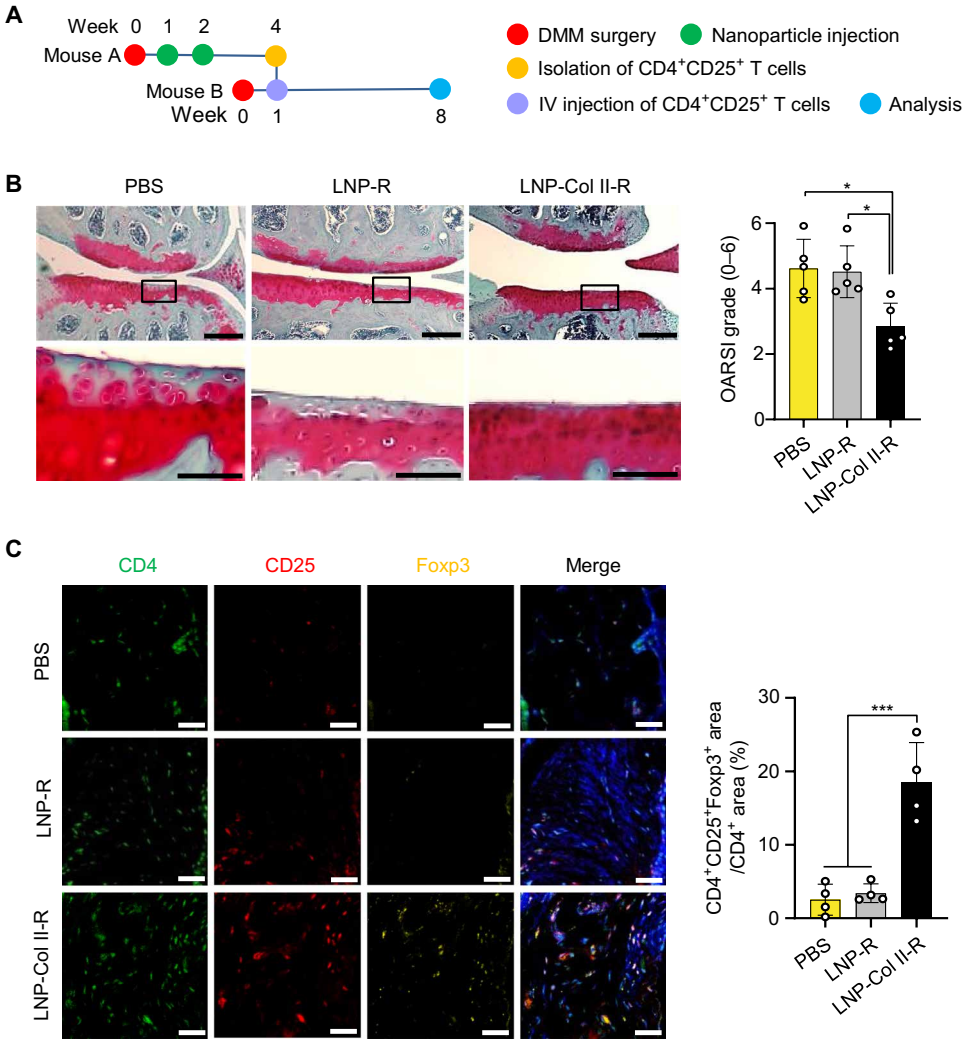

Fig. 7. Therapeutic effects of adoptive transfer of CD4$^+$CD25$^+$ T cells to OA mice. CD4$^+$CD25$^+$ T cells were isolated from mice treated with intradermal injection of PBS, LNP-R, or LNP-Col II-R. (**A**) Timeline of the experiment. (**B**) Representative Safranin O–Fast Green–stained sections of the cartilages and the OARSI grade 8 weeks after adoptive cell transfer. Photographs of the bottom row are higher magnification of the rectangular areas of those in the top row. Scale bars, 100 μm ($n = 5$). (**C**) Immunostaining of T_{regs} in the synovium. Scale bars, 20 μm ($n = 4$). (B and C) *$P < 0.05$ and ***$P < 0.001$. One-way ANOVA (multiple comparison) with Tukey's post hoc test.

the other groups (Fig. 7C). These data suggest that T_{regs} induced by LNP-Col II-R injection are likely responsible for the therapeutic effects of LNP-Col II-R.

To determine whether CD11c$^+$ DCs induced by LNP-Col II-R injection could alleviate OA, we performed adoptive DC transfer to OA mice. CD11c$^+$ DCs were isolated from the right iLNs of mice that had been treated with intradermal injection of PBS, LNP-R, or LNP-Col II-R. The isolated CD11c$^+$ cells were transferred to OA mice by intradermal injection. Safranin O–Fast Green staining of the joints at 8 weeks indicated that the LNP-Col II-R group showed less destruction in the cartilage and significantly lower OARSI grade than the other groups (fig. S7).

Toxicity of LNP-Col II-R

The cytotoxicity and in vivo organ toxicity of LNP-Col II-R were evaluated. DCs were treated with PBS, free Col II, or LNP-Col II-R in vitro for 24 hours. The number of viable cells (fig. S8) and the mRNA levels of apoptosis-related genes [Bcl-2–associated X protein (BAX) and caspase-3] (fig. S9) were not different among all the groups. Intradermal injection of LNP-Col II-R into mice did not exhibit toxicity to organs, as the blood serum levels of alanine aminotransferase (ALT), aspartate aminotransferase (AST), blood urea nitrogen (BUN), and creatinine were not changed by the injection (fig. S10). Furthermore, histological examination of the major organs at 8 weeks showed no signs of organ damage or inflammation (fig. S11). The results indicated that LNP-Col II-R did not cause cytotoxicity or organ toxicity.

DISCUSSION

The OA pathology is heterogeneous and involves several factors, such as genetic, hormone- or age-related intrinsic factors, and traumatic injury–induced extrinsic factors (*43*, *44*). Considering the heterogeneity of OA pathology, the proposed treatment may not be effective for OA as a whole and could specifically be effective for injury-induced inflammatory OA. Inflammatory immune cells, such as T_H1 cells,

T_H17 cells, and M1 macrophages, in OA joints contribute to local inflammation, cartilage destruction, and pain. In OA progression, inflammatory immune cells secrete proinflammatory cytokines such as IL-1β, TNF-α, and IFN-γ, which induce chondrocyte apoptosis (*45*) and stimulate chondrocytes to produce cartilage matrix–degrading enzymes [e.g., MMP13 and a disintegrin and metalloproteinase 5 (ADAMTS5)] (*46*). As OA progresses, the number of inflammatory immune cells, which infiltrate OA joints and secrete inflammatory cytokines and cartilage matrix–degrading enzymes, increases, which eventually increases damage to cartilage tissues and aggravates the disease. In addition, inflammatory immune cells correlate with pain. Inflammatory immune cells, especially activated M1 macrophages and inflammatory T cells within the synovial membrane and fat pad beneath the patella, were increased in OA patients (*47*). M1 macrophages are known to cause pain in OA by interacting with neurons (*48*). The number of $CD4^+$ T cells within the synovium has also been reported to be related to the pain level (*47*), implying that pain in OA is influenced by the overall inflammatory status within the joint. T_H1 and T_H17 cells intensify pain by secreting inflammatory cytokines and by stimulating inflammatory M1 macrophages, while T_{regs} weaken pain by secreting anti-inflammatory cytokines, especially IL-10 (*49*). Col II–specific T_{regs}, which are generated by LNP-Col II-R injection, can migrate to inflammatory OA joints via chemotaxis and secrete anti-inflammatory cytokines such as IL-10 upon T_{reg} activation via interaction with Col II, a potential autoantigen in OA patients (*8*, *11*, *12*, *23*–*25*), presented on MHC II of APCs (e.g., activated B cells, DCs, and macrophages) in OA synovium. The cytokines secreted from T_{regs} in OA joints can inhibit the inflammatory immune cells (T_H1 cells, T_H17 cells, and M1 macrophages) in OA joints and mitigate the local inflammation, leading to pain relief and cartilage protection.

The LNP-Col II-R therapy inhibited cartilage destruction (Fig. 5B). This may result from both cartilage regeneration (Fig. 5J) and cartilage protection (Fig. 5, G and H) induced by LNP-Col II-R. LNP-Col II-R protected cartilage from destruction by relieving inflammation (Fig. 6) and inhibiting MMP13 expression (Fig. 5, H and I). A number of previous studies have demonstrated cartilage regeneration following resolution of inflammation in OA joints. A previous study demonstrated that removing senescent chondrocytes that secrete proinflammatory cytokines in OA joints in animal models induced cartilage regeneration (*50*). In addition, intraarticular injection of mesenchymal stem cells, which exert anti-inflammatory paracrine action, into OA joints resulted in regeneration of the cartilage (*51*). Inflammation resolution in joints inhibits the nuclear factor κB (NF-κB) signaling pathway in chondrogenic progenitor cells, which up-regulates chondrogenesis (*52*). Reduced levels of inflammatory cytokines recruit more progenitor cells around the site of the OA lesion for active chondrogenesis and decrease MMP13 expression (*46*), which would lead to increases in Col II expression and avoid Col II degradation in the cartilage. Therefore, resolution of local inflammation in OA joint by LNP-Col II-R may lead to cartilage ECM protection and regeneration.

For clinical translation of LNP-Col II-R nanoparticle therapy, human peptide, DNA or mRNA of Col II, or Col II epitope of MHC II can be loaded in LNPs. Meanwhile, this therapy may not be applied to all OA patients. Because OA pathology is heterogeneous and autoantibodies against Col II are found in approximately half of OA patients (*24*), this therapy could be applied to OA patients diagnosed with autoantibodies against Col II.

In summary, here, we suggest tolerogenic nanoparticles that mitigate local inflammation in OA joints as an off-the-shelf treatment modality for OA. A previous study has demonstrated that intradermal injection of tolerogenic nanoparticles led to uptake of myocardial infarction–related antigen-laden nanoparticles by APCs in dermis, APC migration to adjacent lymph nodes, and induction of T_{regs} that subsequently migrated to the infarction area (*53*). Similarly, intradermal injection of LNP-Col II-R nanoparticles generated Col II–specific T_{regs} in vivo (Fig. 4C). A higher number of Col II–specific T_{regs} were observed in the joint of the LNP-Col II-R injection group compared to the other groups (Fig. 6A). $CD4^+CD25^+$ T cells isolated from the spleen of LNP-Col II-R–injected mice and intravenously injected to DMM animals (adoptive T_{reg} transfer) migrated to the diseased joints (Fig. 7C). These results suggest that intradermal injection of LNP-Col II-R leads to induction of antigen-specific T_{regs} that migrate to the target lesion to alleviate the disease. This therapy offers advantages over the current therapies for OA. NSAID treatments and intraarticular injection of hyaluronic acid focus on alleviating symptoms and offer only temporary therapeutic benefit.

Cell therapies for OA, such as autologous chondrocyte implantation and mesenchymal stem cell implantation, are invasive, costly, time-consuming, and complicated. In contrast, LNP-Col II-R nanoparticle therapy not only can relieve pain and prevent cartilage destruction but also is simple, noninvasive, off-the-shelf, and cost-effective. Unlike adoptive transfer of polyclonal T_{regs} that has potential side effects of nonspecific systemic immunosuppression, LNP-Col II-R nanoparticle therapy can avoid the side effects by inducing OA-specific immune tolerance.

Although the LNP-Col II-R nanoparticle therapy showed a therapeutic efficacy in the DMM animal model, the animal model has limitations. While the DMM surgical model is the gold standard in the field (*33*, *43*), the model does not include all of the heterogeneous OA pathologies and is restricted to an initial inflammatory input driven by the surgical insult.

MATERIALS AND METHODS

Collagen peptide preparation

Col II was prepared by treating type II collagen (Chondrex Inc., USA) with collagenase III (STEMCELL Technologies, Canada). In OA development, primarily collagenase III (MMP13) is known to degrade the cartilage matrix. Col II and collagenase III (10 U/ml) were dissolved in 0.05 M acetic acid and PBS, respectively. The solutions were mixed and incubated overnight with stirring. After collagen digestion, the molecular weight of Col II was determined by matrix-assisted laser desorption/ionization time-of-flight (MALDI-TOF) mass spectrometry (Spotlight 400, PerkinElmer, USA).

LNP preparation

LNPs were synthesized with a conventional thin-film hydration method (*54*). Briefly, DOTAP, 1,2-dioleoyl-*sn*-glycero-*e*-phosphethanolamine (DOPE), and 1,2-distearoyl-*sn*-glycero-3-phosphoethanolamine-*N*-[methoxy(polyethylene glycol)-2000] (ammonium salt) (PEG2000 PE) were dissolved in chloroform. Cholesterol and rapamycin were dissolved in 100% pure ethanol. DOTAP, DOPE, cholesterol, and PEG PE were placed in glass vials at a molar ratio of 0.475:0.35:0.12:0.05. Before dehydration, 70 μg of rapamycin was added. The vial was agitated at 40°C until the solvents dried. Then, 100 μg of Col II was added to the vial. PBS was added for hydration until the total volume

became 1 ml. The hydrated solution was serially extruded through 1-μm, 400-nm, and 200-nm pore size filters.

Nanoparticle characterization

The shape of LNPs was characterized with transmission electron microscopy (TEM) [JEM-F200 (TFEG), JEOL Ltd., Japan]. The size and zeta potential of LNPs were determined by dynamic laser scattering (DLS) (Zetasizer Nano ZS, Malvern Panalytical, UK). For size analysis, LNPs were hydrated in PBS. For zeta potential analysis, LNPs were hydrated in PBS, followed by dialysis. Dialysis was required to substitute the PBS solution with distilled water. As Col II was reconstituted in acetic acid and hydrated in PBS solution, the zeta potential could be influenced by the mixed solutions. Therefore, dialysis after extrusion was necessary. To evaluate the colloidal stability of LNPs, the size variation of LNPs was monitored for 3 days by DLS. The entrapment efficiency and release profile of rapamycin in LNPs were confirmed by HPLC. Briefly, the temperature of the column was maintained at 60°C. For the mobile phase, 10 mM ammonium acetate and acetonitrile were used (25:75, v/v). The flow rate was 1.5 ml/min, and 5 μl of samples was injected for each measurement. LNP-R was destroyed with 0.1% Triton X-100 for 10 min to determine the amount of rapamycin actually loaded in LNPs. Last, the entrapment efficiency (%) was calculated according to the following equation: (The amount of rapamycin actually loaded in LNPs/The amount of rapamycin added to LNPs) × 100. To determine the release profile of Col II loaded in LNP-Col II-R, bicinchoninic acid (BCA) protein assay was performed.

Isolation of BMDCs

Bone marrow–derived dendritic cells (BMDCs) were isolated from 6-week-old female C57BL/6 mice (OrientBio, Gyeonggi, South Korea). After proper trimming, the tops of both the femur and tibia were cut and placed in two Eppendorf tubes that were stacked together. The tip of the inner smaller tube was holed using an 18-gauge needle. The tubes were spun at 13,500 rpm for 1 min. The isolated bone marrow cells were reconstituted in RPMI 1640 medium containing 10% fetal bovine serum, penicillin (100 U/ml), streptomycin (100 μg/ml), 50 μM 2-mercaptoethanol (Sigma-Aldrich, USA), and 20 μg of recombinant murine granulocyte macrophage colony-stimulating factor (PeproTech, USA). The solution was filtered through a 70-μm cell strainer. Cells were plated in a 100-mm dish at a concentration of 2×10^5 cells/ml and cultured. After 3 days, 10 ml of fresh medium was added. DCs collected at day 10 were used for further experiments (*55*).

Nanoparticle addition to DC cultures

One million DCs were seeded in each well of a six-well plate. For nanoparticle uptake evaluation, LNPs were labeled with 1,1′-dioctadecyl-3,3,3′,3′-tetramethylindocarbocyanine perchlorate (DiI) (Invitrogen, USA), added to DC cultures, and incubated for 24 hours. DCs were washed twice with PBS and fixed with 4% paraformaldehyde (PFA). The nuclei were stained with 4′,6-diamidino-2-phenylindole (DAPI) (Vector Laboratories, USA). For Col II uptake and presentation on DCs, Col II was labeled with *N*-hydroxysuccinimide (NHS)–fluorescein isothiocyanate (FITC) (Thermo Fisher Scientific, USA) before addition to DC cultures. Cell cytoplasm was stained with CellMask (Thermo Fisher Scientific, USA). To detect the Eα peptide (52 to 68) (AnaSpec Inc., USA) on MHC II of DCs, free Eα or LNP-Eα-R–treated DCs were stained with I-Ab monoclonal antibodies (Invitrogen, USA). The staining results were examined with a confocal laser scanning microscope (LSM710, Carl Zeiss, Germany). For tDC induction, DCs were cocultured with different kinds of LNPs for 48 hours and activated by LPS (200 ng/ml) for 24 hours. To mimic the in vivo inflammatory environment in OA, DCs were treated with LPS in vitro in the tDC induction studies (Fig. 2, D to F). DCs were stained with peridinin chlorophyll protein (PerCP)/cyanine 5.5–labeled anti-mouse CD40 (BioLegend, USA, 124617), phycoerythrin (PE)–labeled anti-mouse CD80 (BioLegend, USA, 104707), allophycocyanin-labeled anti-mouse CD86 antibodies (BioLegend, USA, 105011), and PE/cyanine 5–labeled anti-mouse MHC II (BioLegend, USA, 107612) for flow cytometry analysis (FACSAria II, BC Biosciences, USA). At the same time, the mRNA levels of TNF-α and TGF-β in the cells were evaluated with the qRT-PCR StepOnePlus Real-Time PCR system (Applied Biosystems, CA, USA). The primers used for mRNA level analysis are listed in table S1. ELISA was conducted to measure the secretion level of TNF-α (BioLegend, USA) and TGF-β (Invitrogen, USA) from DCs that are treated with different kinds of LNPs.

Biodistribution of nanoparticles after intradermal injection

LNP-Col II-R nanoparticles were labeled with DiR (AAT Bioquest, USA). Briefly, DiR iodide in ethanol at 1 mg/ml was added to the nanoparticle stock solution. DiR-labeled LNP-Col II-R in 100 μl of PBS was injected intradermally into mice. The biodistribution was evaluated by an IVIS spectrum instrument (IVIS SpectrumCT, PerkinElmer, USA). To examine the interaction between DCs and LNP-Col II-R in vivo, LNP-Col II-R nanoparticles were labeled with 1,1′-dioctadecyl-3,3,3′,3′-tetramethylindodicarbocyanine (DiD) (Invitrogen, USA) and injected intradermally into mice. iLNs were harvested 24 hours after injection and cryosectioned. DCs in the iLNs were stained with CD11c antibodies (Abcam, USA, ab33438) and CD3 antibodies (Abcam, USA, ab5690). The coexistence of $CD11c^+$ cells with DiD-labeled LNPs or CD11c and $CD3^+$ cells with DiD-labeled LNPs was analyzed with confocal microscopy.

Antigen-specific T_{reg} induction in vivo and in vitro

Different kinds of LNPs were injected intradermally near the right iLN of OT-II transgenic mice, where $CD4^+$ T cell receptors are specifically responsive to chicken $OVA_{323–339}$. The study with OT-II transgenic mice was approved by the Institutional Animal Care and Use Committee (IACUC) at Seoul National University (SNU-190726). Four days after injection, lymph nodes were harvested and minced for T_{reg} analysis. The gathered cells were stained with mouse anti-CD4–FITC (BioLegend, USA, 116003) and mouse anti-CD25–allophycocyanin antibodies (BioLegend, USA, 101909) for 30 min at 4°C. For intracellular Foxp3 staining, the cells were permeabilized with Fix/Perm buffer (eBioscience, USA) for 30 min at 4°C, washed with permeabilization buffer (eBioscience, USA), and stained with mouse anti-Foxp3–PE antibodies (BioLegend, USA, 126403) for 30 min at 4°C. The cells were analyzed with an automated high-speed flow cytometry system (FACSAria II, BD Biosciences, USA). For in vitro induction of antigen-specific T_{regs}, different kinds of LNPs were treated with DC cultures for 2 days, followed by LPS (200 ng/ml) treatment for 24 hours. The treated DCs were cocultured with $CD4^+$ T cells isolated from OT-II transgenic mice in the presence of TGF-β (2 ng/ml) for another 4 days. OT-II $CD4^+$ T cells were isolated by magnetic-activated cell sorting (MACS) according to the manufacturer's instructions (Miltenyi Biotec, USA). After 4 days of coculture, the

T cells were collected and analyzed for the expression of CD4, CD25, and Foxp3 with FACSAria II. For the induction of antigen-specific T_{regs} in wild-type mice, DMM surgery was conducted, and different kinds of LNPs were treated once a week, three times in total. Four days after the third injection, splenocytes were harvested and seeded in 24-well plates (1×10^6 cells per well). Antigens (12.5 μg/ml) were treated, and the cells were harvested after 72 hours. The cells were stained with anti-CD4, anti-CD25, and anti-Foxp3 antibodies, and the proportion of $CD4^+CD25^+Foxp3^+$ T_{regs} was analyzed with FACSAria II. The mRNA levels of anti-inflammatory cytokines (Foxp3 and TGF-β) were analyzed with qRT-PCR.

DMM surgery–induced OA mouse model

Animal experiments were approved by the IACUC at Seoul National University (SNU-190426-1-3). For OA induction, 10-week-old male C57BL/6 mice (OrientBio, Gyeonggi, South Korea) were anesthetized with ketamine (200 mg/kg) and Rompun (10 mg/kg). Ten-week-old mice were used because several previous animal studies involving OA use the surgically induced OA model in around 10-week-old skeletally mature mice (*56*). Male mice were used in the experiments because the incidence of posttraumatic OA model is higher in the male murine model than in female models (*57*). Female hormones have chondroprotective effects, while male hormones aggravate the disease (*58*). Only the right leg was operated. The skin beneath the tendon of the hindlimb was opened. To secure a clear view and perform delicate operation, the whole step was performed under a microscope. The fat pad was carefully cleared, and the medial meniscus was destabilized with a No. 11 surgical blade. After destabilization, the inner wounded area was closed with coated vicryl polyglactin 910 (Ethicon, USA). The outer skin was closed with nonabsorbable black silk suture (AILEE, USA). The OA-induced mice were randomly grouped ($n = 5$ per group), and 2 mg of nanoparticles (42 μg of rapamycin and 50 μg of Col II peptide per animal) in 100 μl of PBS was injected intradermally at weeks 1, 2, and 6. The nanoparticles were injected intradermally because intradermal injection is simple and noninvasive and previous studies have demonstrated that intradermal injection of tolerogenic nanoparticles resulted in the induction of T_{regs} (*53*). To ameliorate the initial inflammation induced by inflammatory M1 macrophages and effector T cells after DMM surgery, the nanoparticles were injected at weeks 1 and 2. The nanoparticles were injected again at week 6 to boost the induction of Col II–specific T_{regs}. For sham surgical group, only the skin of the right leg was incised and no further procedures were conducted. In previous studies, DMM-induced mice were sacrificed between 4 and 12 weeks (*59*) and mostly at 8 weeks for therapeutic effect evaluation (*60*). Considering that synovial inflammation does not occur in very early stage of OA, we excluded early time points for animal sacrifice and assessed the therapeutic effects at 8 weeks.

Pain evaluation

The pain evaluation was conducted 8 weeks after surgery. For the mechanical allodynia test, each animal was acclimatized in a single chamber for at least 30 min. An electronic von Frey device (Dynamic Plantar Aesthesiometer, Ugo Basile, Italy) was placed beneath the animals, and the filaments pressed the footpad of the animals successively starting from lower force. The point at which the animals felt pain and removed their foot from the plate was recorded. For the static weight-bearing test, each animal was acclimatized in the chamber for at least 5 min. Both forelegs were forced up against the wall of the chamber, and only the hindlimbs were placed on each right and left weighing machine (Incapacitance Meter, IITC Life Science, USA). The results recorded on both sides of the weighing machine were analyzed. The greater the pain perception of the animals, the faster they removed their foot from the plate.

Histology and immunohistochemistry

The joints were harvested 8 weeks after surgery, fixed with 4% PFA for 24 hours, and decalcified in Decalcifying Solution-Lite (Sigma-Aldrich, USA) for 5 days. The samples were embedded in paraffin and serially sectioned frontally at 3-μm thickness using a microtome (Leica RM2125, Germany). For Safranin O–Fast Green staining, the sections were stained with 0.1% Safranin O solution and 0.05% Fast Green solution, mounted with Canada balsam (Sigma-Aldrich, USA), and examined with a microscope (Olympus IX71-22FL/PH, Tokyo, Japan). The stained images were scored by the OARSI scoring method by four observers who were blind to the animal groups, and three slides per joint were used to generate each data point. For assessment of synovitis, the slides were stained with Harris Hematoxylin (Cancer Diagnostics Inc., USA) and Clearview Eosin (BBC Biochemical, USA). Immunostaining for collagen type II α 1 chain (Col2a1) and MMP13 was performed using the EnVision Detection Kit (DAKO Agilent Technologies Inc., USA). Sections were stained with primary antibodies against Col II (Abcam, USA, ab34712) and MMP13 (Abcam, USA, ab3208) at 4°C overnight and incubated with EnVision/horseradish peroxidase (HRP) for 30 min. The final colored products were developed using chromogen diaminobenzidine (DAB) and examined under a microscope (Leica Biosystems, Nussloch, Germany). For immunostaining for T_{regs}, M1 macrophages, and M2 macrophages, tissue sections were stained with anti-CD4–Alexa Fluor 488 (Invitrogen, USA, A-11006), anti-CD25–allophycocyanin (BD Pharmingen, USA, 550874), anti-Foxp3 (Novus, USA, NB100-39002), anti-F4/80 (Abcam, USA, ab16911), anti-iNOS (Abcam, USA, ab15323), and anti-arginase (Novus, USA, NBP1-32731) antibodies. After overnight incubation at 4°C, the sections were incubated with goat anti-rabbit IgG secondary antibody–PE (SouthernBiotech, USA, 4050-09), goat anti-mouse IgG secondary antibody–Alexa Fluor 555 (Invitrogen, USA, A-21127), and goat anti-rabbit IgG secondary antibody–FITC (Novus, USA, NB7182). For immunostaining of IFN-γ–secreting $CD4^+$ T cells, IL-17–secreting $CD4^+$ T cells, IL-1β–secreting M1 macrophages, and IL-10–secreting T_{regs}, tissue sections were stained with anti-CD4 (Novus, USA, NBP2-25191), anti-F4/80 (Abcam, USA, ab16911), anti-Foxp3 (Novus, USA, NB100-39002), anti–IL-1β (Novus, USA, NB600-630), anti–IL-17 (Abcam, USA, ab79056), anti–IFN-γ (Invitrogen, USA, 12-7311-82), and anti–IL-10 (Abcam, USA, ab189392) antibodies. The staining was visualized by confocal microscopy (LSM 700 Meta, Carl Zeiss, Oberkochen, Germany). TUNEL assay was performed using the TUNEL assay kit (DeadEnd fluorometric TUNEL system) according to the manufacturer's instruction (Promega, USA, G3250).

PCR of the whole joint

mRNA levels of inflammatory and anti-inflammatory cytokines in the joints were analyzed. The joint tissues including synovium, femoral condyle, and tibial plateau were harvested, and unnecessary tissues were trimmed as much as possible. The excised tissues were minced with a blade and then homogenized thoroughly. Before homogenization, TRIzol was added, and the samples were stored at −80°C until use. mRNA levels of TNF-α, TGF-β, IL-1β, and IFN-γ were evaluated

with qRT-PCR. The primers used for mRNA level analysis are listed in table S1.

Adoptive transfer of T_{regs} to OA mice

$CD4^+CD25^+$ T cells were isolated from the spleens of OA mice that had been treated with intradermal injection of PBS, LNP-R, or LNP-Col II-R at weeks 1 and 2. The isolated splenocytes were stained with anti-CD4–FITC (BD Pharmingen, USA, 450042-82) and anti-CD25–allophycocyanin (BioLegend, USA, 102012) for 30 min at 4°C in the dark. $CD4^+CD25^+$ T cells were sorted by Moflo (Beckman Coulter, Brea, CA, USA). The sorted $CD4^+CD25^+$ T_{regs} (0.5×10^6 cells per animal) were transferred to OA mice through intravenous injection. Eight weeks after T_{reg} transfer, the joints were harvested for analysis.

Adoptive transfer of $CD11c^+$ DCs to OA mice

$CD11c^+$ DCs were isolated from the right iLNs of wild-type mice that had been treated with intradermal injections of PBS, LNP-R, or LNP-Col II-R on weeks 1 and 2. The isolated lymphocytes were stained with anti-CD11c MicroBeads UltraPure (Miltenyi Biotec, USA, 130-125-835) for 15 min and sorted by MACS bead column according to the manufacturer's instruction (Miltenyi Biotec, USA). The sorted $CD11c^+$ DCs (0.5×10^6 cells per animal) were transferred to OA mice through intradermal injection. Eight weeks after DC transfer, the joints were harvested for analysis.

In vitro and in vivo toxicity of LNP-Col II-R

For cytotoxicity analysis, DCs were cocultured with LNP-Col II-R nanoparticles for 24 hours, and the numbers of viable cells were determined using the cell counting kit-8 (CCK-8) assay (EZ-CyTox, DogenBio, Korea) according to the manufacturer's instructions. mRNA levels of BAX and caspase-3 were determined by qRT-PCR. The primers used for the mRNA level analysis are shown in table S1. For in vivo organ toxicity analysis, 2 mg of LNP-Col II-R nanoparticles was intradermally injected into mice. At various time points, blood serum samples were isolated, and the blood levels of ALT, AST, BUN, and creatinine were determined with a veterinary automatic dry chemistry analyzer (DRI-CHEM 3500s, Fuji, Japan). At week 8, major organs, including the heart, liver, lung, kidney, and spleen, were harvested and processed for histological examination with H&E staining method.

Statistical analysis

Unless stated otherwise, data are presented as means ± SD. The data were analyzed by one-way analysis of variance (ANOVA) with Tukey's post hoc test. Differences were considered statistically significant when $P < 0.05$.

SUPPLEMENTARY MATERIALS

Supplementary material for this article is available at https://science.org/doi/10.1126/sciadv.abo5284

View/request a protocol for this paper from *Bio-protocol*.

REFERENCES AND NOTES

1. O. De Lucia, A. Murgo, F. Pregnolato, I. Pontikaki, M. De Souza, A. Sinelli, R. Cimaz, R. Caporali, Hyaluronic acid injections in the treatment of osteoarthritis secondary to primary inflammatory rheumatic diseases: A systematic review and qualitative synthesis. *Adv. Ther.* **37**, 1347–1359 (2020).
2. R. L. Davies, N. J. Kuiper, Regenerative medicine: A review of the evolution of autologous chondrocyte implantation (ACI) therapy. *Bioengineering (Basel)* **6**, 1–16 (2019).
3. H. Kim, B.-K. Lee, Anti-inflammatory effect of adipose-derived stromal vascular fraction on osteoarthritic temporomandibular joint synoviocytes. *Tissue Eng. Regen. Med.* **17**, 351–362 (2020).
4. M. J. Wood, A. Leckenby, G. Reynolds, R. Spiering, A. G. Pratt, K. S. Rankin, J. D. Isaacs, M. A. Haniffa, S. Milling, C. M. Hilkens, Macrophage proliferation distinguishes 2 subgroups of knee osteoarthritis patients. *JCI Insight* **4**, 1–12 (2019).
5. W. H. Robinson, C. M. Lepus, Q. Wang, H. Raghu, R. Mao, T. M. Lindstrom, J. Sokolove, Low-grade inflammation as a key mediator of the pathogenesis of osteoarthritis. *Nat. Rev. Rheumatol.* **12**, 580–592 (2016).
6. M. J. Benito, D. J. Veale, O. FitzGerald, W. B. Van Den Berg, B. Bresnihan, Synovial tissue inflammation in early and late osteoarthritis. *Ann. Rheumat. Dis.* **64**, 1263–1267 (2005).
7. B. Moradi, P. Schnatzer, S. Hagmann, N. Rosshirt, T. Gotterbarm, J. P. Kretzer, M. Thomsen, H.-M. Lorenz, F. Zeifang, T. Tretter, $CD4^+CD25^+/^{high}$ $CD127^{low/-}$ regulatory T cells are enriched in rheumatoid arthritis and osteoarthritis joints—Analysis of frequency and phenotype in synovial membrane, synovial fluid and peripheral blood. *Arthritis Res. Ther.* **16**, 1–13 (2014).
8. G. H. Yuan, K. Masuko-Hongo, T. Kato, K. Nishioka, Immunologic intervention in the pathogenesis of osteoarthritis. *Arthritis Rheum.* **48**, 602–611 (2003).
9. E. B. P. Lopes, A. Filiberti, S. A. Husain, M. B. Humphrey, Immune contributions to osteoarthritis. *Curr. Osteoporos. Rep.* **15**, 593–600 (2017).
10. Y. S. Li, W. Luo, S. A. Zhu, G. H. Lei, T cells in osteoarthritis: Alterations and beyond. *Front. Immunol.* **8**, 1–10 (2017).
11. M. Sakata, K. Masuko-Hongo, H. Nakamura, H. Onuma, J. Tsuruha, H. Aoki, K. Nishioka, T. Kato, Osteoarthritic articular chondrocytes stimulate autologous T cell responses in vitro. *Clin. Exp. Rheumatol.* **21**, 704–710 (2003).
12. R. R. Da, Y. Qin, D. Baeten, Y. Zhang, B cell clonal expansion and somatic hypermutation of Ig variable heavy chain genes in the synovial membrane of patients with osteoarthritis. *J. Immunol.* **178**, 557–565 (2007).
13. A. Haseeb, T. M. Haqqi, Immunopathogenesis of osteoarthritis. *Clin. Immunol.* **146**, 185–196 (2013).
14. H. Du, K. Masuko-Hongo, H. Nakamura, Y. Xiang, C.-D. Bao, X.-D. Wang, S.-L. Chen, K. Nishioka, T. Kato, The prevalence of autoantibodies against cartilage intermediate layer protein, YKL-39, osteopontin, and cyclic citrullinated peptide in patients with early-stage knee osteoarthritis: Evidence of a variety of autoimmune processes. *Rheumatol. Int.* **26**, 35–41 (2005).
15. M. M. Tiemessen, A. L. Jagger, H. G. Evans, M. J. van Herwijnen, S. John, L. S. Taams, $CD4^+CD25^+Foxp3^+$ regulatory T cells induce alternative activation of human monocytes/macrophages. *Proc. Natl. Acad. Sci. U.S.A.* **104**, 19446–19451 (2007).
16. J. L. Coombes, N. J. Robinson, K. J. Maloy, H. H. Uhlig, F. Powrie, Regulatory T cells and intestinal homeostasis. *Immunol. Rev.* **204**, 184–194 (2005).
17. S. S. Duffy, B. A. Keating, G. Moalem-Taylor, Adoptive transfer of regulatory T cells as a promising immunotherapy for the treatment of multiple sclerosis. *Front. Neurosci.* **13**, 1–5 (2019).
18. M. Romano, G. Fanelli, C. J. Albany, G. Giganti, G. Lombardi, Past, present, and future of regulatory T cell therapy in transplantation and autoimmunity. *Front. Immunol.* **10**, 1–14 (2019).
19. Y. C. Kim, A.-H. Zhang, Y. Su, S. A. Rieder, R. J. Rossi, R. A. Ettinger, K. P. Pratt, E. M. Shevach, D. W. Scott, Engineered antigen-specific human regulatory T cells: Immunosuppression of FVIII-specific T- and B-cell responses. *Blood* **125**, 1107–1115 (2015).
20. K. V. Tarbell, S. Yamazaki, K. Olson, P. Toy, R. M. Steinman, $CD25^+CD4^+$ T cells, expanded with dendritic cells presenting a single autoantigenic peptide, suppress autoimmune diabetes. *J. Exp. Med.* **199**, 1467–1477 (2004).
21. X. Xie, M. A. van Delft, F. Shuweihdi, S. R. Kingsbury, L. A. Trouw, G. M. Doody, P. G. Conaghan, F. Ponchel, Auto-antibodies to post-translationally modified proteins in osteoarthritis. *Osteoarthr. Cartil.* **29**, 924–933 (2021).
22. M. Wang, E. R. Sampson, H. Jin, J. Li, Q. H. Ke, H.-J. Im, D. Chen, MMP13 is a critical target gene during the progression of osteoarthritis. *Arthritis Res. Ther.* **15**, 1–11 (2013).
23. T. Takagi, H. E. Jasin, Interactions between anticollagen antibodies and chondrocytes. *Arthritis Rheum.* **35**, 224–230 (1992).
24. L. I. Sakkas, C. D. Platsoucas, The role of T cells in the pathogenesis of osteoarthritis. *Arthritis Rheum.* **56**, 409–424 (2007).
25. L. S. Lohmander, L. M. Atley, T. A. Pietka, D. R. Eyre, The release of crosslinked peptides from type II collagen into human synovial fluid is increased soon after joint injury and in osteoarthritis. *Arthritis Rheum.* **48**, 3130–3139 (2003).
26. J. O. Eloy, R. Petrilli, J. F. Topan, H. M. R. Antonio, J. P. A. Barcellos, D. L. Chesca, L. N. Serafini, D. G. Tiezzi, R. J. Lee, J. M. Marchetti, Co-loaded paclitaxel/rapamycin liposomes: Development, characterization and in vitro and in vivo evaluation for breast cancer therapy. *Colloids Surf. B Biointerfaces* **141**, 74–82 (2016).
27. S. Stoll, J. Delon, T. M. Brotz, R. N. Germain, Dynamic imaging of T cell-dendritic cell interactions in lymph nodes. *Science* **296**, 1873–1876 (2002).

28. J. C. Huh, D. H. Strickland, F. L. Jahnsen, D. J. Turner, J. A. Thomas, S. Napoli, I. Tobagus, P. A. Stumbles, P. D. Sly, P. G. Holt, Bidirectional interactions between antigen-bearing respiratory tract dendritic cells (DCs) and T cells precede the late phase reaction in experimental asthma: DC activation occurs in the airway mucosa but not in the lung parenchyma. *J. Exp. Med.* **198**, 19–30 (2003).
29. V. Mundra, R. I. Mahato, Design of nanocarriers for efficient cellular uptake and endosomal release of small molecule and nucleic acid drugs: Learning from virus. *Front. Chem. Sci. Eng.* **8**, 387–404 (2014).
30. S. Rayamajhi, J. Marchitto, T. D. T. Nguyen, R. Marasini, C. Celia, S. Aryal, pH-responsive cationic liposome for endosomal escape mediated drug delivery. *Colloids Surf. B Biointerfaces* **188**, 110804 (2020).
31. R. Fischer, H. R. Turnquist, T. Taner, A. W. Thomson, Use of rapamycin in the induction of tolerogenic dendritic cells, in *Dendritic Cells*, G. Lombardi, Y. Riffo-Vasquez, Eds. (Springer, 2009), vol. 188.
32. O. Snir, J. Bäcklund, J. Boström, I. Andersson, J. Kihlberg, J. H. Buckner, L. Klareskog, R. Holmdahl, V. Malmström, Multifunctional T cell reactivity with native and glycosylated type II collagen in rheumatoid arthritis. *Arthritis Rheum.* **64**, 2482–2488 (2012).
33. S. S. Glasson, T. J. Blanchet, E. A. Morris, The surgical destabilization of the medial meniscus (DMM) model of osteoarthritis in the 129/SvEv mouse. *Osteoarthr. Cartil.* **15**, 1061–1069 (2007).
34. C. Little, A. Barai, D. Burkhardt, S. Smith, A. Fosang, Z. Werb, M. Shah, E. Thompson, Matrix metalloproteinase 13–deficient mice are resistant to osteoarthritic cartilage erosion but not chondrocyte hypertrophy or osteophyte development. *Arthritis Rheum.* **60**, 3723–3733 (2009).
35. S. Glasson, M. Chambers, W. Van Den Berg, C. Little, The OARSI histopathology initiative–Recommendations for histological assessments of osteoarthritis in the mouse. *Osteoarthr. Cartil.* **18**, S17–S23 (2010).
36. C. L. Wu, J. McNeill, K. Goon, D. Little, K. Kimmerling, J. Huebner, V. Kraus, F. Guilak, Conditional macrophage depletion increases inflammation and does not inhibit the development of osteoarthritis in obese macrophage Fas-induced apoptosis–Transgenic mice. *Arthritis Rheumatol.* **69**, 1772–1783 (2017).
37. C. S. Bonnet, D. A. Walsh, Osteoarthritis, angiogenesis and inflammation. *Rheumatology* **44**, 7–16 (2005).
38. F. Berenbaum, Osteoarthritis as an inflammatory disease (osteoarthritis is not osteoarthrosis!). *Osteoarthr. Cartil.* **21**, 16–21 (2013).
39. B. J. de Lange-Brokaar, A. Ioan-Facsinay, G. J. van Osch, A. M. Zuurmond, J. Schoones, R. E. Toes, T. W. Huizinga, M. Kloppenburg, Synovial inflammation, immune cells and their cytokines in osteoarthritis: A review. *Osteoarthr. Cartil.* **20**, 1484–1499 (2012).
40. A. Mathiessen, P. G. Conaghan, Synovitis in osteoarthritis: Current understanding with therapeutic implications. *Arthritis Res. Ther.* **19**, 18 (2017).
41. B. D. Singer, L. S. King, F. R. D'Alessio, Regulatory T cells as immunotherapy. *Front. Immunol.* **5**, 1–10 (2014).
42. W. Xu, Q. Lan, M. Chen, H. Chen, N. Zhu, X. Zhou, J. Wang, H. Fan, C.-S. Yan, J.-L. Kuang, Adoptive transfer of induced-Treg cells effectively attenuates murine airway allergic inflammation. *PLOS ONE* **7**, 1–10 (2012).
43. D. G. Manlapaz, G. Sole, P. Jayakaran, C. M. Chapple, Risk factors for falls in adults with knee osteoarthritis: A systematic review. *Am. J. Phys. Med. Rehabil.* **11**, 745–757 (2019).
44. M. Henriksen, L. B. Jørgensen, J. Aaboe, Obesity and walking: Implications for knee osteoarthritis and plantar heel pain. *Curr. Obes. Rep.* **1**, 160–165 (2012).
45. T. Aizawa, T. Kon, T. Einhorn, L. Gerstenfeld, Induction of apoptosis in chondrocytes by tumor necrosis factor-alpha. *J. Orthop. Res.* **19**, 785–796 (2001).
46. Q. Hu, M. Ecker, Overview of MMP-13 as a promising target for the treatment of osteoarthritis. *Int. J. Mol. Sci.* **22**, 1–22 (2021).
47. D. N. Greif, D. Kouroupis, C. J. Murdock, A. J. Griswold, L. D. Kaplan, T. M. Best, D. Correa, Infrapatellar fat pad/synovium complex in early-stage knee osteoarthritis: Potential new target and source of therapeutic mesenchymal stem/stromal cells. *Front. Bioeng. Biotechnol.* **8**, 1–16 (2020).
48. T. Geraghty, D. R. Winter, R. J. Miller, R. E. Miller, A.-M. Malfait, Neuroimmune interactions and osteoarthritis pain: Focus on macrophages. *Pain Rep.* **6**, 1–12 (2021).
49. A. Kavelaars, C. J. Heijnen, T cells as guardians of pain resolution. *Trends Mol. Med.* **27**, 302–313 (2021).
50. O. H. Jeon, C. Kim, R.-M. Laberge, M. Demaria, S. Rathod, A. P. Vasserot, J. W. Chung, D. H. Kim, Y. Poon, N. David, Local clearance of senescent cells attenuates the development of post-traumatic osteoarthritis and creates a pro-regenerative environment. *Nat. Med.* **23**, 775–781 (2017).
51. Y. B. Park, C. W. Ha, C. H. Lee, Y. C. Yoon, Y. G. Park, Cartilage regeneration in osteoarthritic patients by a composite of allogeneic umbilical cord blood-derived mesenchymal stem cells and hyaluronate hydrogel: Results from a clinical trial for safety and proof-of-concept with 7 years of extended follow-up. *Stem Cells Transl. Med.* **6**, 613–621 (2017).
52. M. Li, R. Xiao, J. Li, Q. Zhu, Regenerative approaches for cartilage repair in the treatment of osteoarthritis. *Osteoarthr. Cartil.* **25**, 1577–1587 (2017).
53. S. P. Kwon, B. H. Hwang, E. H. Park, H. Y. Kim, J. R. Lee, M. Kang, S. Y. Song, M. Jung, H. S. Sohn, E. Kim, Nanoparticle-mediated blocking of excessive inflammation for prevention of heart failure following myocardial infarction. *Small* **17**, 2101207 (2021).
54. M. J. Copland, M. A. Baird, T. Rades, J. L. McKenzie, B. Becker, F. Reck, P. C. Tyler, N. M. Davies, Liposomal delivery of antigen to human dendritic cells. *Vaccine* **21**, 883–890 (2003).
55. A. Madaan, R. Verma, A. T. Singh, S. K. Jain, M. Jaggi, A stepwise procedure for isolation of murine bone marrow and generation of dendritic cells. *J. Biol. Methods* **1**, 1–6 (2014).
56. R. F. Loeser, A. L. Olex, M. A. McNulty, C. S. Carlson, M. F. Callahan, C. M. Ferguson, J. Chou, X. Leng, J. S. Fetrow, Microarray analysis reveals age-related differences in gene expression during the development of osteoarthritis in mice. *Arthritis Rheum.* **64**, 705–717 (2012).
57. P. Van der Kraan, Factors that influence outcome in experimental osteoarthritis. *Osteoarthr. Cartil.* **25**, 369–375 (2017).
58. H.-L. Ma, T. Blanchet, D. Peluso, B. Hopkins, E. Morris, S. Glasson, Osteoarthritis severity is sex dependent in a surgical mouse model. *Osteoarthr. Cartil.* **15**, 695–700 (2007).
59. J. Hu, J. Zhou, J. Wu, Q. Chen, W. Du, F. Fu, H. Yu, S. Yao, H. Jin, P. Tong, Loganin ameliorates cartilage degeneration and osteoarthritis development in an osteoarthritis mouse model through inhibition of NF-κB activity and pyroptosis in chondrocytes. *J. Ethnopharmacol.* **247**, 1–8 (2020).
60. J.-H. Kim, G. Lee, Y. Won, M. Lee, J.-S. Kwak, C.-H. Chun, J.-S. Chun, Matrix cross-linking–Mediated mechanotransduction promotes posttraumatic osteoarthritis. *Proc. Natl. Acad. Sci. U.S.A.* **112**, 9424–9429 (2015).

Acknowledgments

Funding: This work was supported by a grant (2019M3A9H1103651) from the National Research Foundation of Korea funded by the Ministry of Science and ICT, Republic of Korea, and by a grant (HV22C0069) from the Korea Health Technology R&D Project through the Korea Health Industry Development Institute (KHIDI), funded by the Ministry of Health and Welfare, Republic of Korea. **Author contributions:** H.S.S., J.W.C., J.J., M.-L.C., and B.-S.K. analyzed data and wrote the manuscript. H.S.S. conducted cell culture and animal studies. H.S.S. and J.W.C. conducted immunostaining. H.S.S., J.J., and H.S.N. performed cell isolation and adoptive T_{reg} transfer. H.S.S., S.Y., and J.-H.K. conducted pain tests. H.S.S. and S.P.K. performed flow cytometry and nanoparticle characterization. H.S.S. and M.J. conducted DMM surgery on animals. M.-L.C. and B.-S.K. were responsible for the conception and the experimental design. All authors participated in editing and approval of the final text of the manuscript. **Competing interests:** The authors declare that they have no competing interests. **Data and materials availability:** All data needed to evaluate the conclusions in the paper are present in the paper and/or the Supplementary Materials.

Submitted 14 February 2022
Accepted 6 October 2022
Published 25 November 2022
10.1126/sciadv.abo5284